This is an Accepted Manuscript for *Journal of Glaciology*. Subject to change during the editing and production process.
DOI: 10.1017/jog.2024.33

The stepwise decrease of 4+ year ice extent and its linked survivability since around 2007

Qi Shan[1,3], Ke Fan[2]*, and Jiping Liu[2]

[1]Institute of Atmospheric Physics, Chinese Academy of Sciences, Beijing, 100029, China

[2]School of Atmospheric Sciences, Sun Yat-sen University, and Southern Marine Science and Engineering Guangdong Laboratory (Zhuhai), Zhuhai, 519082, China

[3]University of the Chinese Academy of Sciences, Beijing, 100049, China

Corresponding author: Ke Fan (fank8@mail.sysu.edu.cn)

Abstract

Recent studies have reported a shift in the Arctic sea ice to a younger state after around 2007. This study reveals that this shift can be primarily attributed to a stepwise-type reduction in the extent of four years or older (4+ year) ice and its linked survivability. After this shift, the fraction of 4+ year ice extent relative to the total ice changed from 30.5% to 10.0%. Sea ice survivability can serve as a key indicator of sea ice persistence in response to other factors. We demonstrate that the decrease of 4+ year ice is controlled by the decrease of its linked survivability in a nonlinear manner, signifying small alterations in the survivability can result in relatively large changes in the extent of 4+ year ice. The decrease in survivability is affected by both the winter and summer processes. Summer melting contributed the most, while the contribution of the export through Fram Strait was minor. However, the significant rise in residual loss during the growth season suggests that other winter processes may also have played an important role.

https://doi.org/10.1017/jog.2024.33 Published online by Cambridge University Press

1 Introduction

Sea ice is critical in the energy budget and the exchange of heat and momentum between the atmosphere and ocean, and thus the ecosystem in the Arctic (Thomas, 2017). Based on whether it has survived at least one summer melt season, sea ice can be classified into two categories: first-year ice (FYI) and multi-year ice (MYI). Due to longer growth periods and more deformation processes, MYI is thicker, stronger, less salty, and rougher than FYI (Bi and others, 2020). These contrasting characteristics may lead to divergent feedback mechanisms and climate implications.

During the past few decades, the Arctic sea ice coverage has shrunk rapidly, with a faster rate of loss for the MYI than for the total ice (Maslanik and others, 2011; Comiso, 2012; Liu and others, 2019). Investigating the changes and underlying drivers of MYI coverage is of great importance. On the one hand, sea ice age can be used as a proxy for thickness (Maslanik and others, 2007; Tschudi and others, 2016). This correspondence can also be supported by the strong correlation between the MYI area and the total ice volume in the satellite product (Kwok, 2018). On the other hand, the decrease in MYI could provide more area for seawater to freeze into FYI during winter (Zhao and others, 2023).

The changes in MYI coverage can be considered as controlled by its survivability, which describes the likelihood of sea ice persisting throughout a growth-melt cycle (Armour and others, 2011; Tooth and Tschudi, 2018). The survivability serves as an indicator of sea ice response to climate forcing. For the MYI coverage, the survivability can be affected by both thermodynamic and dynamic processes, including summer melting, export through Fram Strait (FS), and ridging (e.g., Kwok, 2007, 2015; Kwok and Cunningham, 2010; Babb and others, 2023, hereafter B23; Regan and others, 2023), but separating their respective contributions is challenging.

In addition to gradually shrinking in response to global warming, emerging studies indicate the Arctic sea ice can show stepwise-type regime shifts. Sumata and others (2023) revealed an abrupt stepwise shift around 2007 from an “old, thick, deformed ice regime” to a “younger, thinner, more uniform ice regime” in the Arctic by continuous monitoring data in

https://doi.org/10.1017/jog.2024.33 Published online by Cambridge University Press

FS since 1990. Moore and others (2022) reported a similar shift in the western Arctic sea ice. Additionally, B23 found that the MYI area experienced two stepwise reductions in 1989 and around 2007, respectively. They indicated that the former reduction was primarily driven by export, while the latter was attributed to a combination of export, melt, and replenishment. Moreover, this regime shift around 2007 is also manifested in other aspects of Arctic climate, including an intensified response of the volume flux through FS to variation in Arctic sea ice volume after 2007 (Yang and others, 2023) and a transition in Arctic Dipole mode from a near-neutral phase to a positive phase around 2007 (Polyakov and others, 2023).

In this study, we will first show another stepwise variation around 2007, that is, the decrease of the extent of sea ice aged four years or older (4+ year ice) in the Arctic Basin, and demonstrate how it is controlled by the decrease of survivability. Subsequently, we will estimate the individual contribution of various processes to the decrease of survivability. The paper is structured as follows. Section 2 presents the data employed and the definition of sea ice survivability. Section 3 introduces how we budget sea ice survivability. Section 4 outlines the results of our analysis. Section 5 gives a discussion of our results. The final section provides a summary.

2 Data and method

2.1 Data

Here we use version 4 of the sea ice age (SIA) dataset from the National Snow and Ice Data Center (NSIDC; Tschudi and others, 2019a). The NSIDC-SIA dataset is derived by tracking ice parcels in a Lagrangian sense using sea ice motion (SIM) data and recording their age. In particular, each grid cell that contains ice in NSIDC-SIA data was advected and tracked as a Lagrangian parcel at weekly time steps. If the sea ice concentration (SIC) at each grid cell is greater than or equal to 15% throughout the entire melt season, the grid cell is considered to have survived the summer melting, and its age increases by one. Therefore, SIA will add one at the end of summer, and it is a discrete value. Furthermore, if several ice parcels propagated into the same grid cell, the age of the oldest parcel is assigned to that grid cell. The version 4 NSIDC-SIA dataset has eliminated errors created by artificial ice

https://doi.org/10.1017/jog.2024.33 Published online by Cambridge University Press

divergence in the previous version (Tschudi and others, 2020). Furthermore, Ye and others (2023) have demonstrated its ability to generally discriminate between MYI and FYI. The dataset we used is in a 12.5 × 12.5 km Equal-Area Scalable Earth (EASE) grid and available weekly from 1984 to 2022. The distribution of SIA during the period 1985–2022 is illustrated in Figure 1 and our analysis will be limited to the Arctic Basin defined in the bottom right corner of Figure 1, as MYI predominantly exist in this region.

We also use the NSIDC SIM (Tschudi and others, 2019b) and SIC (DiGirolamo and others, 2022) datasets. The SIM and the SIC data are originally in a 25 × 25 km EASE grid and NSIDC polar stereographic grid, respectively. Both datasets were then interpolated using the bilinear method to 12.5 × 12.5 km EASE grid, facilitating subsequent calculations with SIA. The SIM data are weekly as the SIA data, while the SIC data are every other day from October 26, 1978 to July 9, 1987 and daily afterwards. Additionally, monthly 2m temperature and sea level pressure in the fifth-generation global reanalysis produced by ECMWF (ERA5; Hersbach and others, 2020) were used in this study.

2.2 Sea ice survivability

The week that SIA increases (hereafter called the start week) varies each year (Figure S1), with an average occurring around the 37th week. We defined one growth-melt cycle as from the start week to the week preceding the start week in the following year. The increase in SIA for a specific ice parcel signifies its survival over the last growth-melt cycle. Following Armour and others (2011), we can estimate sea ice survivability by the survival ratio of sea ice extent (SIE), which is expressed as follows:

$$\beta_{i,\,n} = SIE_{i+1,\,(n,\,St^{th})} / SIE_{i,\,(n-1,\,St^{th})} \tag{1}$$

Where i is the age of ice, n is the year, the $\beta_{i,\,n}$ represents the survival ratio of ice aged i in year n, and the $SIE_{i+1,\,(n,\,St^{th})}$ represents the extent of sea ice aged i+1 in the start week of year n. For example, if all the 2 year ice in the start week of 1999 can persist until the start week of 2000 and become 3 year ice. The ratio between $SIE_{3,\,(2000,\,St^{th})}$ and $SIE_{2,\,(1999,\,St^{th})}$ is 1, i.e., the survival ratio of 2 year ice in 2000 $(\beta_{2,\,2000})$.

https://doi.org/10.1017/jog.2024.33 Published online by Cambridge University Press

The survival ratio in one complete growth-melt cycle, $\beta_{i,\ n}$, can be further divided into the survival ratio in the growth season, $\beta_{i,\ n}^{growth}$, and the survival ratio in the melt season, $\beta_{i,\ n}^{melt}$. It is found the total SIE in the Arctic Basin begins to decrease around the 18th week (Figure S2), indicating the onset of the melt season. Considering that MYI typically melts later than FYI, we have chosen a slightly later period, the 20th–25th weeks, as the boundary between the growth and melt seasons to reduce the sample error (the results are not sensitive to the windows selected here). Then the survival ratio in the growth and melt seasons can be calculated as follows:

$$\beta_{i,\ n}^{growth} = SIE_{i,\ (n,\ \overline{20^{th}-25^{th}})} / SIE_{i,\ (n-1,\ St^{th})} \tag{2}$$

$$\beta_{i,\ n}^{melt} = SIE_{i+1,\ (n,\ St^{th})} / SIE_{i,\ (n,\ \overline{20^{th}-25^{th}})} \tag{3}$$

Where the $SIE_{i,\ (n,\ \overline{20^{th}-25^{th}})}$ represents the extent of sea ice aged i averaged over the 20th–25th weeks of year n. Therefore, we will have $\beta_{i,\ n} = \beta_{i,\ n}^{growth} \times \beta_{i,\ n}^{melt}$.

3. Budget of sea ice survivability

As mentioned in Section 1, sea ice survivability can be influenced by various processes. Here, we mainly focused on the contributions of two processes, summer melting and export through FS, to the loss of MYI extent, while the remaining loss was considered as residual. Furthermore, the budget of total loss during one growth-melt cycle was divided into two parts, growth season and melt season, respectively, as indicated by the following equation:

$$Loss_{i,\ n} = \underbrace{\frac{Export^{growth} + \mathrm{Re}sidual^{growth}}{Loss^{growth}}}_{} + \underbrace{\frac{Export^{melt} + Melting + \mathrm{Re}sidual^{melt}}{Loss^{melt}}}_{} \tag{4}$$

where the $Loss_{i,\ n}$ is the loss of i year ice extent in n year, the superscript *growth* and *melt* represent the corresponding loss in the growth and melt season, respectively. Greater $Loss_{i,\ n}$ corresponds to lower $\beta_{i,\ n}$, as demonstrated by $\beta_{i,\ n} = 1 - Loss_{i,\ n} / SIE_{i,\ (n-1,\ St^{th})}$. Similar to section 2,2, we use the 20th–25th weeks as the boundary between the growth and melt seasons when calculating the loss of MYI extent. For example, the melt analyzed in this paper is the

https://doi.org/10.1017/jog.2024.33 Published online by Cambridge University Press

average of melt calculated by treating each week within the 20th–25th weeks as an individual boundary.

3.1 Sea ice export through FS

We select a zonal gate at 80°N (17°W–16°E, red line in the bottom right corner of Figure 1) to calculate the sea ice area fluxes through FS (note that we do not consider the concentration in the calculation). In the calculation, we divide the gate into small segments with a resolution of 1° (around 20 km). To reduce the sample error in determining the SIA of each segment, we select the nearest four SIA grid cells of each segment and calculate the area fluxes through each segment using the following equations:

$$F_i = \sum_{j=1}^{4} V_{i,j} L / 4 \tag{5}$$

Where F_i is the area export fluxes of i year ice, j represents the number of four nearest grids for each segment, V represents velocity perpendicular to the segment (here is the meridional velocity) calculated from the NSIDC SIM dataset (Tschudi and others, 2019b), L is the length of each segment. The total area fluxes through FS are obtained by summing up the fluxes of each segment. The results are not sensitive to the resolution of segments and the number of nearest grid cells (not shown).

3.2 Summer melting

Since quantifying the melt is a challenging task, here we use an indirect method to estimate it. As we can see, sea ice within the summer minimum SIE will turn into MYI at the onset of the growth season (see the 40th week in Figure 1). While after movement during the growth season, the position of those MYI can change significantly (compare the SIA and the black lines in the 10th week in Figure 1). Some of them were outside of the summer minimum SIE edge of that year (compare the SIA and the white lines in the 10th week in Figure 1), such as in 2007 and 2010. If those MYI keep being outside during the melt season, we can approximate that they were lost due to melt. Therefore, MYI grid cells outside the summer minimum SIE at the onset of melt season (20th–25th weeks in our paper) will be used to

https://doi.org/10.1017/jog.2024.33 Published online by Cambridge University Press

estimate the MYI melt, assuming the MYI inflow and outflow through the summer minimum SIE edge are close during the melt season. We consider this assumption suitable for estimating melt based on the following two points. First, we found that the MYI extent within the summer minimum SIE edge changes mildly after the 25th week compared to our estimated melt in most years. Second, the estimated melt remains relatively stable in the calculation. When using individual weeks from the 15th–30th as the onset of the melt season for calculation, we found that the range of calculated melt is moderate comparing the results using the average of the 20th–25th weeks. Importantly, regardless of the chosen weeks (15th–30th weeks), the difference in average melt before and after 2007, as focused on in section 4.3, remains similar in magnitude.

In our estimation method, a key factor is the relative position between the location of MYI at the onset of the melt season and the summer minimum SIE edge. The shrinkage of the summer minimum SIE edge to a certain degree signifies an intensification of the summer melting process, which can be attributed to thinner ice and warmer temperatures. Simultaneously, the location of the MYI during the melt season is also a crucial factor in determining whether it will disappear due to summer melting. For example, for the same MYI, it is much more likely to melt in the southern Beaufort Sea than in the central Arctic, especially in recent decades. Consequently, the transport of MYI during the growth season can also influence the MYI summer melting by adjusting the location of MYI at the onset of the melt season. Overall, the MYI melt estimated above is actually the combined interaction of dynamic and thermal processes.

This perception is analogous to the melt estimation method in Kwok and Cunningham (2010) and the "survival zone" concept in Mallett and others (2021). Kwok and Cunningham (2010) have employed a novel method to estimate the MYI melt area in the Beaufort Sea. They propagate MYI pixels from 1 April using daily ice motion fields and regarded pixels as melting if they are located outside the daily ice edge after propagation. Mallett and others (2021) define a "survival zone" as the area where sea ice is present on 1 September in more than 50% of the years over the last decade. They suppose that the unusually high export of

https://doi.org/10.1017/jog.2024.33 Published online by Cambridge University Press

MYI during the winter of 2020/21 to areas outside this survival zone (primarily the Beaufort Sea) might lead to greater MYI loss.

It should be noted that the actual MYI melt will be greater than our estimates, as our method does not account for MYI melt within the summer minimum SIE edge, which is associated with reduced SIC. This limitation will be further discussed in Section 5.

3.3 The residual term

The residual term may be composed of the influences of several factors, including the omission of the sea ice export through other gates, such as the Nares Strait (see B23 for the estimations of export through other gates), the bias of our calculation in section 3.1 and 3.2, the sea ice deformation process, along with other artificial or physical biases that we have not considered. Regarding the sea ice deformation, the convergence of MYI reduces its extent, while simultaneously opening seawater and producing FYI during the growth season. The role of deformation process is also highlighted by Regan and others (2023) and considered as a sink in their MYI area budget using a sea ice model. For the NSIDC-SIA dataset used here, we consider the MYI deformation and its effect on FYI production to be common. Specifically, the production of FYI can occur across most regions within MYI coverage (Figure S3 provides an example of 2015/16) and can even be pronounced in the north of the Canadian Arctic Archipelago (CAA), where the oldest ice is situated (refer to section 4.3 and Figure S6). This may, to some extent, underscore the widespread occurrence and impact of MYI deformation.

4. Results

4.1 The stepwise shift of 4+ year ice extent in the Arctic Basin

Figures 2a and S4 show the evolution of the annual average (average over one growth-melt cycle) SIE of different ages during 1985–2022. From the perspective of linear trend during the whole period, a striking feature is the drastic and significant decreasing trend in the extent of 4+ year ice, with a rate of -0.82×10^6 km^2/decade ($p < 0.01$; Figure 2a). The extent of 3 year ice shows a non-significant decreasing trend, whereas the extent of 2 year ice

https://doi.org/10.1017/jog.2024.33 Published online by Cambridge University Press

exhibits a significant ($p < 0.05$) but moderate increasing trend (Figure S4). This results in a non-significant trend in the extent of 2–3 year ice (Figure 2a). Therefore, the evident decline in the MYI coverage reported in previous studies (e.g., Comiso, 2012; B23) might be primarily driven by the decline in the 4+ year ice. As mentioned previously, due to the below-freezing temperature, the greatly reduced MYI extent can be occupied by newly-formed FYI in winter. Therefore, there is a significant increasing trend in the FYI extent, with a rate of 0.49×10^6 km^2/decade ($p < 0.01$; Figure 2a), which can largely offset the decrease of MYI, and thus limit the total loss of sea ice.

However, it is noteworthy that the changes of FYI and 4+ year ice extent are not gradual; instead, they exhibit stepwise characteristics before and after around 1990 and 2008, respectively. After the stepwise changes, the equilibrium states of FYI and 4+ year ice extent (gray dash lines in Figure 1a), which represent the mean state of the sea ice system after adjusting to climate forcing (Armour and others, 2011), have transitioned significantly from the former to the latter. The former stepwise change has been reported in many previous studies, which emphasize the key role of a shift in the Arctic Oscillation (AO) to high index conditions (e.g., Belchansky and others, 2004; B23). The rise in the AO flushed MYI out of the Beaufort Gyre and into Transpolar Drift Stream, leading to increased MYI export. The latter stepwise change, which is the main focus of our investigation, has also been raised in recent studies (e.g., Sumata and others, 2023) and can be clearly identified using the 7-year moving t-test (Figure 2b; similar results are obtained using 9-year and 11-year windows). After this stepwise shift, the FYI extent increased approximately from 3.0×10^6 km^2 to 3.9×10^6 km^2, with its fraction relative to the total ice changing from 42.5% to 61.4%. Meanwhile, the extent of 4+ year ice decreased approximately from 2.1×10^6 km^2 to 0.6×10^6 km^2, with its fraction changing from 30.5% to 10.0%.

The shift towards younger Arctic sea ice after 2008 is also evident in the SIA spatial distribution, as shown in Figures 2c–e. For the 4+ year ice, a noticeable decrease is observed across almost the entire western Arctic (0°–180°W). Its decrease in the north of Greenland and the CAA has been primarily offset by an increase in 2-3 year ice in that region. while its

https://doi.org/10.1017/jog.2024.33 Published online by Cambridge University Press

decrease in the pacific Arctic (purple box in Figure 2c, e) has been primarily offset by an increase in FYI. Additionally, the 2-3 year ice exhibits a decrease in the Arctic Ocean more toward Eurasia, which has been offset by an increase in FYI there. The dipole feature of the change in 2-3 year ice eventually explains a non-significant trend of its extent (Figure 2a). Overall, after this stepwise shift, sea ice in most regions of the Arctic has been occupied by younger ice, with the most pronounced changes in the Pacific Arctic (purple box in Figure 2c, e).

4.2 The control from the decreased survivability

Considering the increase of FYI as an offset to the decline of MYI, which is primarily attributed to the loss of 4+ year ice, our focus here will be on exploring the stepwise decrease of 4+ year ice extent. In the previous subsection, we mentioned that there was no significant trend in the extent of 3 year ice during 1985–2022, whereas the extent of 4+ year ice showed a significant decline after 2008. Therefore, we can reasonably speculate that it is the decrease of survivability that drives less sea ice entering or remaining in the 4+ year ice. As described in section 2.2, we can calculate the survival ratio of 3+ year ice extent $\beta_{3^+,\,n}$ and its counterpart in growth season $\beta_{3^+,\,n}^{growth}$ and melt season $\beta_{3^+,\,n}^{melt}$. We will have:

$$SIE_{4^+,\,(n,\,St^{th})} = \beta_{3^+,\,n} \times SIE_{3^+,\,(n-1,\,St^{th})} \tag{6}$$

Figures 3a and 3b show the evolution of three survival ratios during 1985–2022 and their 7-year moving t-test results. It is evident that the $\beta_{3^+,\,n}$ exhibit stepwise decrease since 2007, which is one-year earlier than the shift year of the annual average SIE of 4+ year ice (see Figure 2b; i.e., 2008). Indeed, this one-year-earlier relationship is expected. According to equation (6), it is the survival ratio in the n year ($\beta_{3^+,\,n}$) that determines the 4+ year ice extent at the onset of $n+1$ year ($SIE_{4^+,\,(n,\,St^{th})}$), which can highly capture the variability of the annual average 4+ year ice extent in the $n+1$ year (their correlation coefficients are 0.99 and 0.93 for non-detrend and detrended time series). During 1989–2006, the mean state of $\beta_{3^+,\,n}$ stood at about 71.7%. However, it significantly decreased to 47.0% after 2007 ($p < 0.01$, two-

https://doi.org/10.1017/jog.2024.33 Published online by Cambridge University Press

sample t-test). The stepwise decrease of $\beta_{3^+,\,n}$ was mainly driven by the decrease of its melt season counterpart $\beta^{melt}_{3^+,\,n}$, which also exhibited a stepwise decrease since 2007. The $\beta^{growth}_{3^+,\,n}$ also exhibit a significant stepwise decrease, albeit three years later (around 2010), thus contributing to the decrease of $\beta_{3^+,\,n}$ as well. Additionally, it is noteworthy that enhanced inter-annual variability has also been observed in all survivability metrics since 2007 (Figure 3a). The decrease of $\beta^{growth}_{3^+,\,n}$ and $\beta^{melt}_{3^+,\,n}$ suggest the combined impact of dynamic and thermodynamic processes on the decrease of $\beta_{3^+,\,n}$. The contribution of specific processes will be estimated in the next subsection. Subsequently, we will quantify the relationship between the stepwise decrease of $SIE_{4^+,\,(n,\,St^{th})}$ and $\beta_{3^+,\,n}$.

Firstly, we have

$$SIE_{3^+,\,(n-1,\,St^{th})} = SIE_{3,\,(n-1,\,St^{th})} + SIE_{4^+,\,(n-1,\,St^{th})}. \tag{7}$$

Following Armour and others (2011), we can decompose each variable into equilibrium and perturbation components: $A_n = \overline{A} + A'_n$. The equilibrium represents the mean state before and after the shift mentioned above. The perturbation represents deviations from the equilibrium state, equivalent to interannual variations. Substituting (7) into (6) and considering only the equilibrium state, we will have

$$\overline{SIE_{4^+,\,St^{th}}} = \overline{SIE_{3,\,St^{th}}} \times \frac{\overline{\beta_{3^+}}}{1-\overline{\beta_{3^+}}}. \tag{8}$$

The equation (8) reveals a non-linear relationship between $\overline{SIE_{4^+,\,St^{th}}}$ and $\overline{\beta_{3^+}}$. This non-linear relationship signifies that the reduction rate in the $\overline{SIE_{4^+,\,St^{th}}}$ could be several times greater than the reduction rate in the $\overline{\beta_{3^+}}$. Specifically, for the equilibrium state of 1989–2006, where the $\overline{\beta_{3^+}} = 71.7\%$, the $\overline{SIE_{4^+,\,St^{th}}}$ will be 2.53 times the $\overline{SIE_{3,\,St^{th}}}$. In comparison, for the equilibrium state of 2007–2022, where the $\overline{\beta_{3^+}} = 47.0\%$, the $\overline{SIE_{4^+,\,St^{th}}}$ will reduce to only 0.89 times the $\overline{SIE_{3,\,St^{th}}}$. With the equation (8), we can reconstruct the $\overline{SIE_{4^+,\,St^{th}}}$ over 1990–

https://doi.org/10.1017/jog.2024.33 Published online by Cambridge University Press

2007 and 2008–2022 by substituting $\overline{SIE_{3,\ St^{th}}}$ and $\overline{\beta_{3^+}}$ into it. Given that the extent of 3 year ice exhibits no significant trend, its average value over 1985–2022 was used to substitute for the $\overline{SIE_{3,\ St^{th}}}$. Then the $\overline{\beta_{3^+}}$ in periods over 1989–2006 and 2007–2022 were substituted into the equation (8), respectively, to obtain the $\overline{SIE_{4^+,\ St^{th}}}$ in their corresponding periods. The outcomes indicate that the reconstructed $\overline{SIE_{4^+,\ St^{th}}}$ can capture the shift observed between two periods (Figure 3c), validating the equation (8) and highlighting the role of decreased $\overline{\beta_{3^+}}$ in controlling the decline of $\overline{SIE_{4^+,\ St^{th}}}$.

Figure 3d shows the net loss/replenishment of 4+ year ice extent ($SIE_{4^+,\ (n,\ St^{th})} - SIE_{4^+,\ (n-1,\ St^{th})}$), which predominantly displays characteristics of interannual oscillations. These oscillations are possibly related to the negative feedback of SIE (Notz and Marotzke, 2012), where most strong negative year-to-year change in SIE is followed by a positive year-to-year change and vice versa. Notably, a sustained net loss is observed during the period 2004–2010. Here, this period could be considered as a transition period from a regime with relatively high $\overline{\beta_{3^+}}$ (1989–2006) to a regime with relatively low $\overline{\beta_{3^+}}$ (2007–2022). Specifically, lower $\overline{\beta_{3^+}}$ represents greater loss and less replenishment for the 4+ year ice extent. As a result, the 4+ year ice extent must reduce to a certain degree to achieve a balance between its loss and replenishment, thereby maintaining an equilibrium state as demonstrated by the equation (8). Therefore, rather than regarding the sustained loss during 2004–2010 as a cause, it is the relatively low $\overline{\beta_{3^+}}$ since 2007 that has controlled or maintained the relatively low 4+ year ice extent.

4.3 The contribution of various processes on the decrease of survivability

Then how have various processes contributed to the decrease of $\overline{\beta_{3^+}}$ since 2007? As described in section 3, we will first illustrate the MYI loss of each SIA due to export through FS and summer melting (Figure 4), and then focus on their loss rate concerning the budget of

https://doi.org/10.1017/jog.2024.33 Published online by Cambridge University Press

$\overline{\beta_{3+}}$ (loss divided by $SIE_{3+,\,(n-1,\,St^{th})}$; Figure 5).

The average annual area export of total ice (including MYI and FYI) through the FS is about 0.75 × 10^6 km^2 (Figure 4a), with MYI accounting for 66% (0.50 × 10^6 km^2). This proportion closely aligns with the findings (67%) reported by Wang and others (2022), although they identify the MYI based on satellite products during 2002–2020. Additionally, the results are not sensitive to the location of the gate (Figure S5). Notably, since around 2007, the 2–3 year ice flux has dominated the MYI flux, while the flux of 4+ year ice accounts for only a minor proportion. Furthermore, over our study period, the MYI proportion in export through FS decreased significantly at a rate of −4% (p = 0.015; not shown). Therefore, the ice export through FS has become younger, which could be due to the contraction of MYI away from FS towards the north of CAA (B23; Krumpen and others, 2019).

For the MYI loss due to summer melting, its annual average is about 0.32 × 10^6 km^2 (Figure 4b). Before around 2010, the MYI melt was mainly 5+ year ice, but after that, it shifted to being primarily composed of 2-3 year ice. In 2013, our estimated MYI melt was extremely low. This is because the summer minimum extent edge in 2013 was more extensive than the previous few years, and simultaneously, few MYI were moving outside of it during the growth season (Figure 1; Perovich and others, 2013). This low melt is consistent with a relatively high sea ice volume in 2013 (Tilling and others, 2015). Again, it is important to note that the estimated MYI melt presented here and below does not account for MYI melt within the summer minimum edge (see Sections 3.2 and 5), and therefore, may underestimate the actual MYI melt area.

Regarding the loss rate driven by the export of 3+ year ice through the FS, no significant trend has been observed since the early 1990s (Figure 5a). Moreover, there is only a modest increase before and after 2007 (12.6% vs 15.4%; Figure 5e), suggesting that the export through FS may not be a primary contributor to the decrease of $\overline{\beta_{3+}}$ since 2007.

For the melt rate of 3+ year ice, there was an evident increase during 2007–2016, although it appeared to rebound back in recent years (Figure 5b). The average melt rate has significantly risen from 4.9% to 14.3% before and after 2007 (Figure 5e). Consequently, we

https://doi.org/10.1017/jog.2024.33 Published online by Cambridge University Press

can attribute the intensified summer melting as a main contributor to the decrease of $\overline{\beta_{3+}}$. As stated in section 3.2, it is worth emphasizing that the estimated melt primarily consists of those 3+ year ice that move to regions that are relatively warm and hard to survive, such as the Beaufort Sea and Chukchi Sea, rather than where they formed. Specifically, during 1989–2006, the summer minimum extent edge is relatively more extensive, and there is only limited 3+ year ice located outside of the edge at the onset of melt season (Figure 6a). Consequently, the amount of melted 3+ year ice is expected to be relatively small. In contrast, after 2007, the summer minimum extent edge has significantly shrunk, especially in the Pacific Arctic (compare the white lines in Figure 6a and 6b), corresponding to intensified melting. However, as a permanent system, the Beaufort Gyre could consistently transport 3+ year ice from the north of CAA to the Beaufort and Chukchi Seas during the growth season. This process can be clearly indicated by the westward extension of the tongue of MYI drawn through the Beaufort Gyre (see shading in Figure 6b and the 10th week in Figure 1). Since the MYI typically cannot survive through the Beaufort Gyre in recent periods (Maslanik and others, 2007; Kwok, 2018; Babb and others, 2022), the loss rate of melt is expected to increase. In addition, the Beaufort Gyre has strengthened during the growth season since 2007, as indicated by the vectors in Figure 6c. This strengthening may be associated to dipole sea level pressure anomaly patterns (contours in Figure 6c) and decreasing ice thickness (Rampal and others, 2009). Consequently, this enhanced Gyre can transport more 3+ year ice to the Beaufort Sea and the Chukchi Sea, where the summer 2m air temperature has warmed noticeably since 2007 (shading in Figure 6c), possibly helping more melt.

The residual loss rate during the growth season shows a noticeable increase after 2011 (Figure 5c), corresponding to the stepwise decrease of $\beta_{3+,n}^{growth}$ since 2010. Before and after 2007, it has increased from 7.7% to 16.5% (Figure 5e), thus also largely contributing to the decrease of $\overline{\beta_{3+}}$. The residual loss rate during the melt season is relatively small compared to its counterpart in the growth season, exhibiting an increase from 3.1% to 6.7% before and after 2007 (Figure 5d and 5e). While the exact causes of the increased residual term remain uncertain, we speculate that increasing sea ice deformation processes, which are related to ice

https://doi.org/10.1017/jog.2024.33 Published online by Cambridge University Press

becoming thinner and more dynamic (Rampal and others, 2009; Zhang and others, 2012), may have played a role. For the MYI, its export through FS and convergence can both reduce its area but produce FYI during winter (see also section 3.3). Since 2011, the FYI production during winter in the Arctic Basin has significantly increased compared to before (Figure 6d). Notably, this increase can even be evident in the north of CAA (Figure S6), where is dominated by the oldest ice in the Arctic. Given that the MYI export through FS exhibits a decreasing trend since 2011 (Figure 4a), we consider that the increased FYI production during winter since 2011 may serve as potential evidence of the strengthened deformation process of MYI, thereby contributing to the increased residual term during the growth season. Detailed examinations of these processes are a promising avenue for future research.

5. Discussion

In the analysis above, we utilized the SIE, which essentially represents the number of corresponding pixels, to quantify the change of 4+ year ice. However, it is important to note that since the SIA was assigned with the oldest parcel within its pixel, the extent of 4+ year ice inherently overestimates its true area. To a certain degree, this bias does hinder our quantitative exploration, such as determining the specific proportion by which the 4+ year ice reduced after 2007. However, for the primary purpose of our study, which is to reflect potential regime shifts around 2007 in the Arctic climate system, we consider this overestimation bias to be acceptable.

Firstly, the shift year (around 2007) derived from 4+ year ice extent aligns well with other studies, such as B23. They also use the NSIDC-SIA dataset, while additionally considering the SIC and using it to calculate the summer minimum MYI area. Second, the loss of 4+ year ice pixels (extent), while not directly indicative of the true reduction in area, does signify that all 4+ years ice parcels within the pixel have been lost by some processes. Therefore, the loss of extent can offer insight into the persistence of pixels containing 4+ years ice. This is also why we employed the sea ice survivability concept from Armour and others (2011) into our analysis, which can reflect the forcing of other factors on the persistence of sea ice, thereby providing insights into changes in Arctic thermodynamic and

https://doi.org/10.1017/jog.2024.33 Published online by Cambridge University Press

dynamic regimes.

Furthermore, we computed the ratio of 3+ year ice pixels with SIC greater than 50% in the start week (Figure 7). We find it can be maintained at relatively high levels (with a minimum of about 84%) despite showing some decline and increased variability since 2000. This indicates that the 3+ years ice pixels we focus on will not be dominated by the physical properties of newly-formed FYI during winter. More importantly, the average ratios between the two periods focused on in our paper (1989–2006 and 2007–2022) are not substantially different (95% vs. 92%). Comparable differences can be achieved by computing the ratio of SIC greater than 60% (92% vs. 88%) or 70% (84% vs. 81%).

We also compared our estimated MYI melt extent with the MYI melt area calculated by B23 (Figure S7). The correlation coefficient between them is 0.63. We attribute this high correlation to two points: first, they both exhibit an increasing trend, and second, their correspondence improves significantly after around 2007. As mentioned in section 3.2, our melt term does not encompass losses associated with reduced SIC within the summer minimum extent. We consider this might be a possible reason for the discrepancy between our melt term and B23 before 2007. During this period, the summer minimum extent is relatively extensive (Figure 6a), and thus the effect of reduced SIC might predominate for the melt term. However, during post-2007, the summer minimum extent has shrunk significantly (Figure 6b), making MYI melt due to propagation to marginal seas, where it is challenging for sea ice to survive the summer transit, more dominant. Based on this comparison, we believe that our estimated older MYI extent loss due to summer melting can reasonably reflect significant changes in the melting process between the periods before and after 2007, although there might be differences compared to the actual melt area.

Overall, given the presence of the overestimation bias, we consider the results obtained in our paper to be semi-quantitative but reasonable. These findings can be helpful for us to understand potential changes in the Arctic climate system within the regime shift around 2007, especially considering the current lack of datasets which can detail the SIC of each age within a pixel. For instance, we propose that the role of summer melting may be more pivotal

https://doi.org/10.1017/jog.2024.33 Published online by Cambridge University Press

than that of FS export in the stepwise decrease of 4+ years ice, although their specific contributions may still entail some uncertainty. Additionally, if long-term datasets similar to Korosov and others (2018), containing corresponding SIC for different ages of sea ice, becomes available in the future, it can be used to validate and complement our study.

6. Summary

Using the NSIDC-SIA dataset, this study revealed that the rapid decline in MYI coverage reported by previous studies (e.g., Kwok, 2018) might be primarily attributed to the decrease in 4+ year ice. Moreover, it is important to emphasize that the 4+ year ice extent decreased stepwise before and after 2008 (2007 summer), instead of decreasing gradually. After this shift, the 4+ year ice extent changed from 2.1×10^6 km^2 to 0.6×10^6 km^2, with its fraction relative to the total ice changing from 30.5% to 10.0%. The shift of SIA towards younger is evident in most regions of the Arctic, with the most pronounced in the Pacific Arctic (purple box in Figure 2c).

The decrease of 4+ year ice extent reflects the fact that less ice entering or remaining in the 4+ year ice group. Therefore, the stepwise decrease of 4+ year ice is essentially a reflection of the reduced survivability of 3+ year ice (the survival part of 3+ year ice will become 4+ year ice in next year), which also decreases stepwise from 72.0% to 46.8% since around 2007. Analyzing the decrease in the 4+ year ice extent from the perspective of survivability provides us with two important insights: (1) when considering the equilibrium state, the 4+ year ice extent is controlled by the survivability of 3+ year ice in a nonlinear manner, as indicated by equation (8). This highlights that small alterations in the survivability can result in relatively large changes in the extent; (2) rather than regarding the sustained loss during 2004–2010 (Figure 2d) as a cause, it is the relatively low survivability since 2007 that has maintained the relatively low 4+ year ice extent, and also has maintained it to not drop to a new lower level.

The decrease in the survivability of 3+ year ice is driven by both the winter and summer processes. The most substantial contribution to the decreased survivability comes from the intensified summer melting (38.1%). The increase in the export through FS is relatively

https://doi.org/10.1017/jog.2024.33 Published online by Cambridge University Press

minor and thus not a major factor. However, the significant rise in residual loss during the growth season suggests that other winter processes, such as sea ice deformation, may have played a significant role in it.

The stepwise decrease in the 4+ year ice extent and its linked survivability could serve as evidence of a regime shift around 2007 within the arctic climate system, as revealed by recent studies (e.g., Sumata and others, 2023; Polyakov and others, 2023). The stepwise variation feature could help to interpret the recent slowdown in the decline of summer arctic sea ice (Francis and Wu, 2020; Zhang, 2021). It is worth noting that the 4+ year ice extent comprises only around 20% of total MYI since 2008, suggesting that an evident decrease in the September sea ice coverage (equivalent to MYI coverage) will need a decrease in the 2–3 year ice.

https://doi.org/10.1017/jog.2024.33 Published online by Cambridge University Press

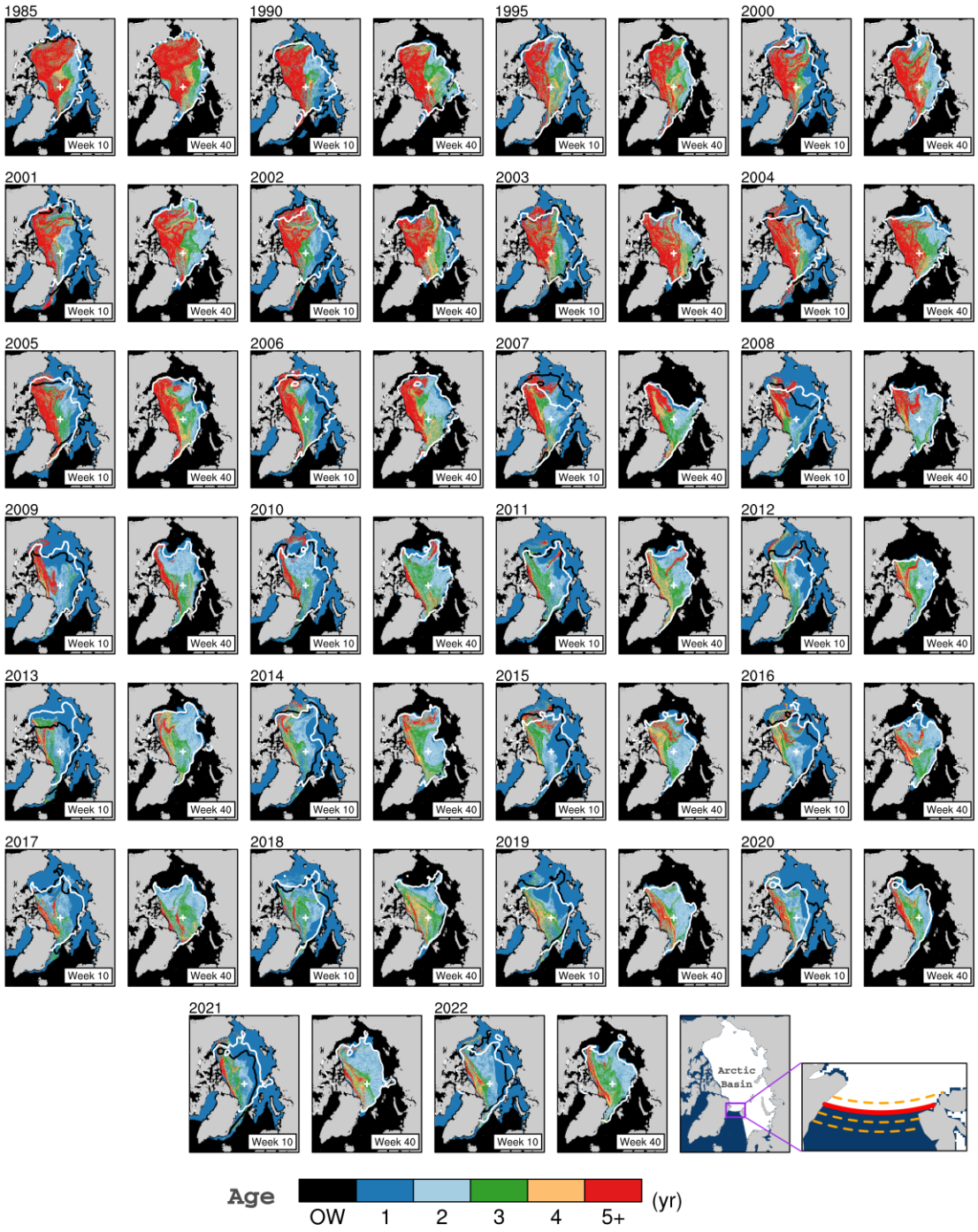

Figure 1. Spatial distribution of Arctic SIA in 10th and 40th weeks during 1985–2022. The distributions before 2000 are presented every five years. The white contours in the 10th and 40th weeks of each year represent the September sea ice edge in the corresponding year, while the black contours in the 10th week represent the September sea ice edge in the previous year. The last two figures in the bottom right corner illustrate the Arctic Basin (white shading) used to analyze in our main text, and the gates used to calculate sea ice area fluxes through FS, respectively. The solid red line indicates the zonal gate at 80°N, while the orange dashed lines represent the zonal gates at 80.5°N, 79.5°N, and 79°N, respectively.

https://doi.org/10.1017/jog.2024.33 Published online by Cambridge University Press

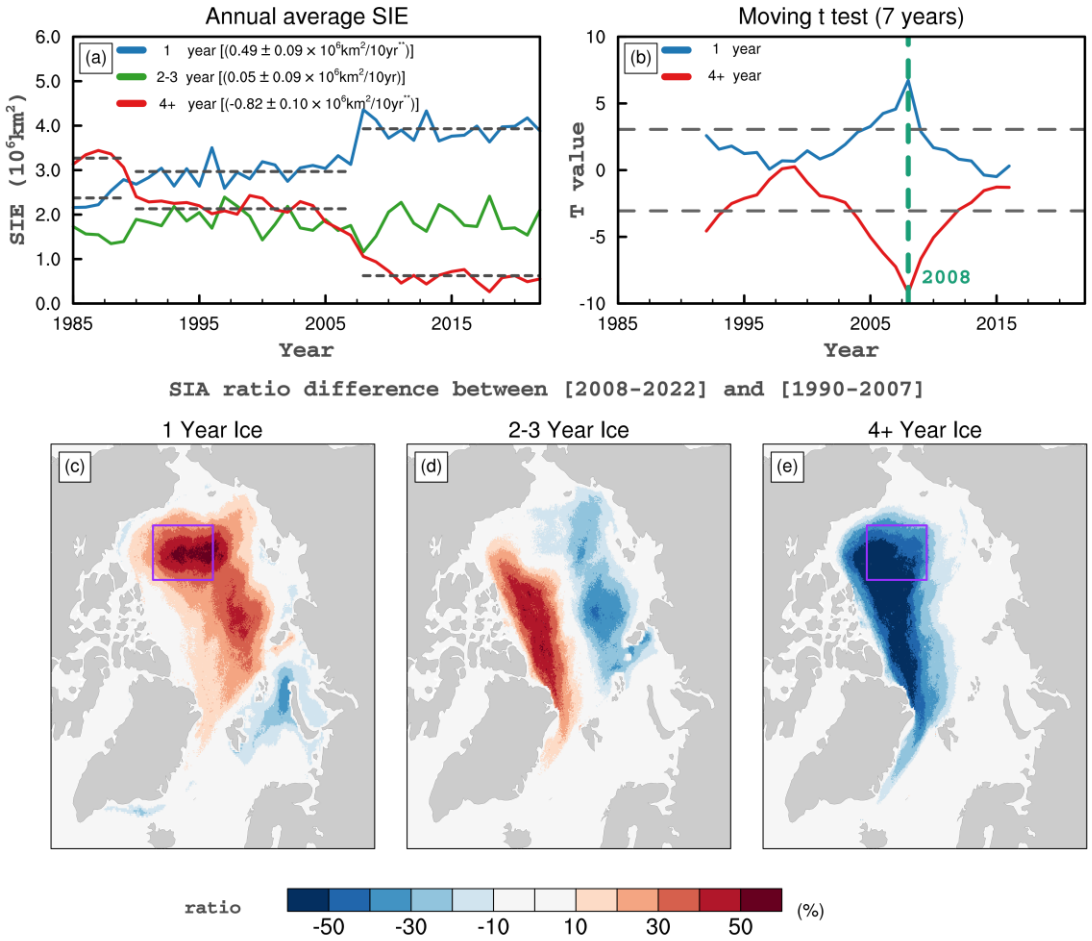

Figure 2. (a) The evolution of the annual average SIE of different ages during 1985–2022. The gray dashed lines represent the equilibrium states of FYI and 4+ year ice during three periods (1985–1989, 1990–2007, and 2008–2022), respectively. The brackets indicate the slopes and their 95% significance limits. One and two asterisks represent the slopes exceeding 95% and 99% significance levels, respectively. (b) The 7 year moving t-test results of 4+ year ice extent and FYI extent. The gray dashed line indicates the 99% significance level. (c–e) The difference in the ratio of each grid cell occupied by certain SIA between 2008–2022 and 1990–2007. The purple box signifies where the 4+ year ice has been obviously replaced by the FYI.

https://doi.org/10.1017/jog.2024.33 Published online by Cambridge University Press

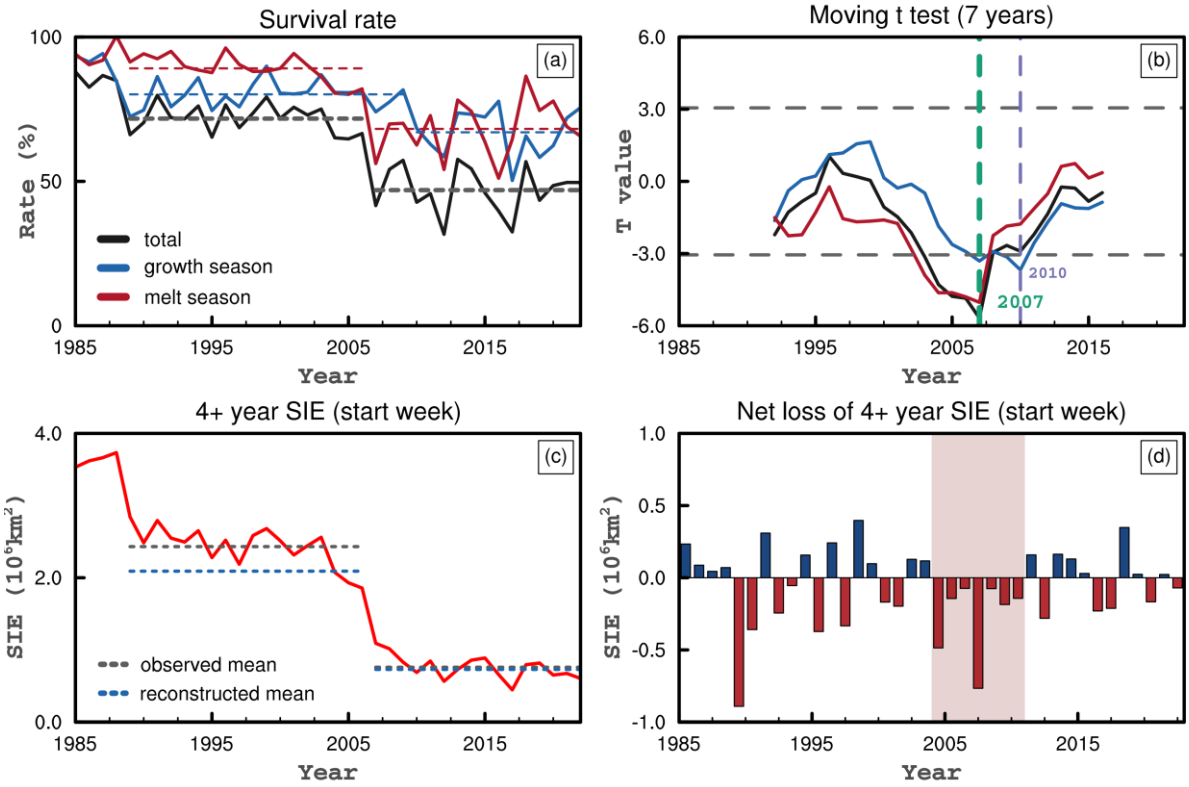

Figure 3. (a) The survival ratio of 3+ year ice in the growth season (blue line), the melt season (red line) and the whole growth-melt cycle (black line) during 1985–2022. The gray and red dashed lines represent the averages of the survival ratio over the periods 1989-2006 and 2007-2022, while the blue dashed line shows the averages for 1989–2009 and 2010–2022. (b) The 7-year moving t test of survival ratio in (a). The gray dashed lines represent the 99% confidence level. (c) The extent of 4+ year ice in the start week during 1985–2022. The gray and blue lines indicate the observed and reconstructed mean of period 1989–2006 and 2007–2022, respectively. (d) The net loss of 4+ year ice extent in the start week. Red shading region represents the period of 2004–2010.

https://doi.org/10.1017/jog.2024.33 Published online by Cambridge University Press

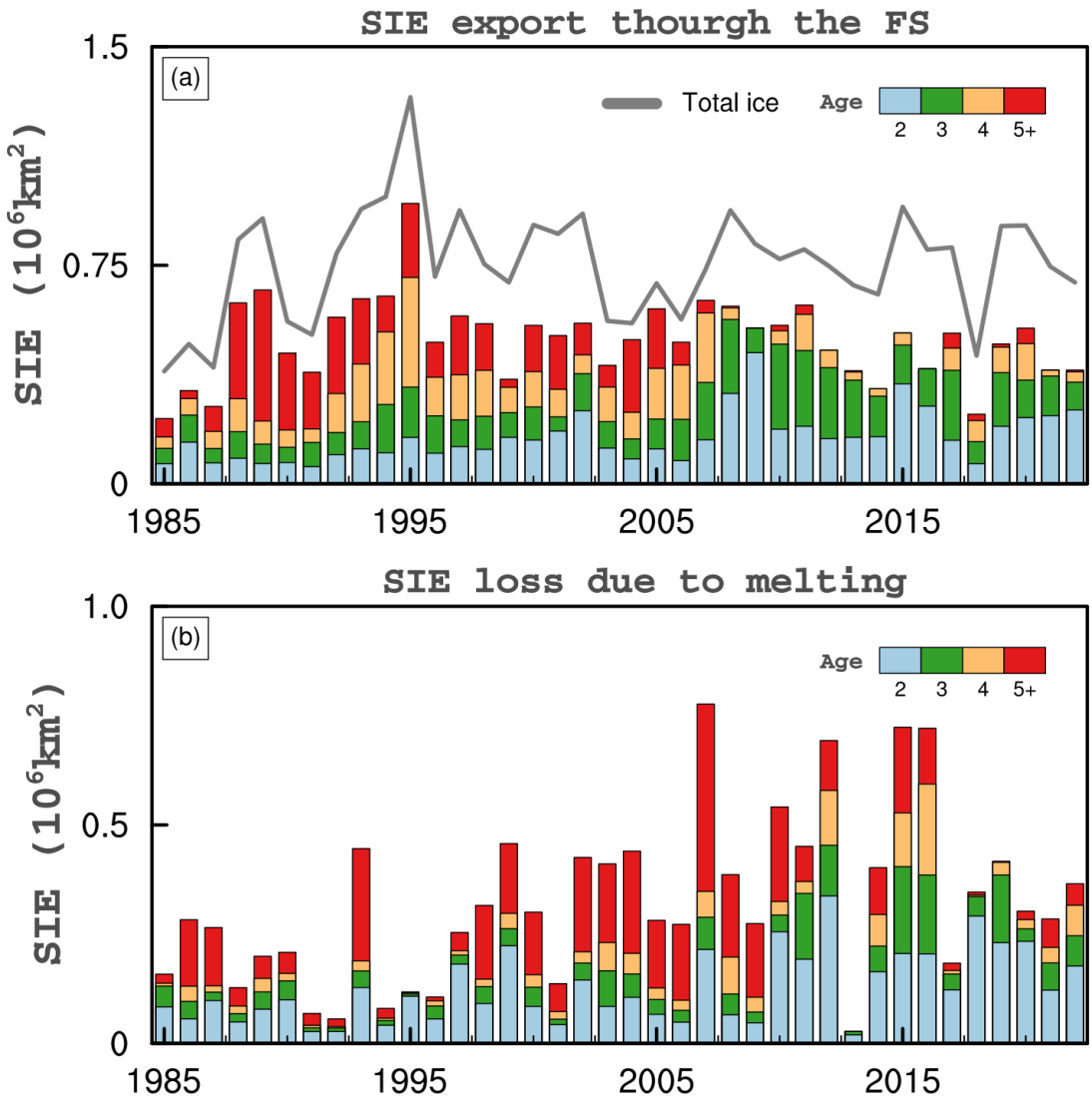

Figure 4. The MYI extent loss due to (a) export through FS and (b) summer melting during 1985–2022. The gray line in (a) indicates the export flux of total ice (FYI and MYI).

https://doi.org/10.1017/jog.2024.33 Published online by Cambridge University Press

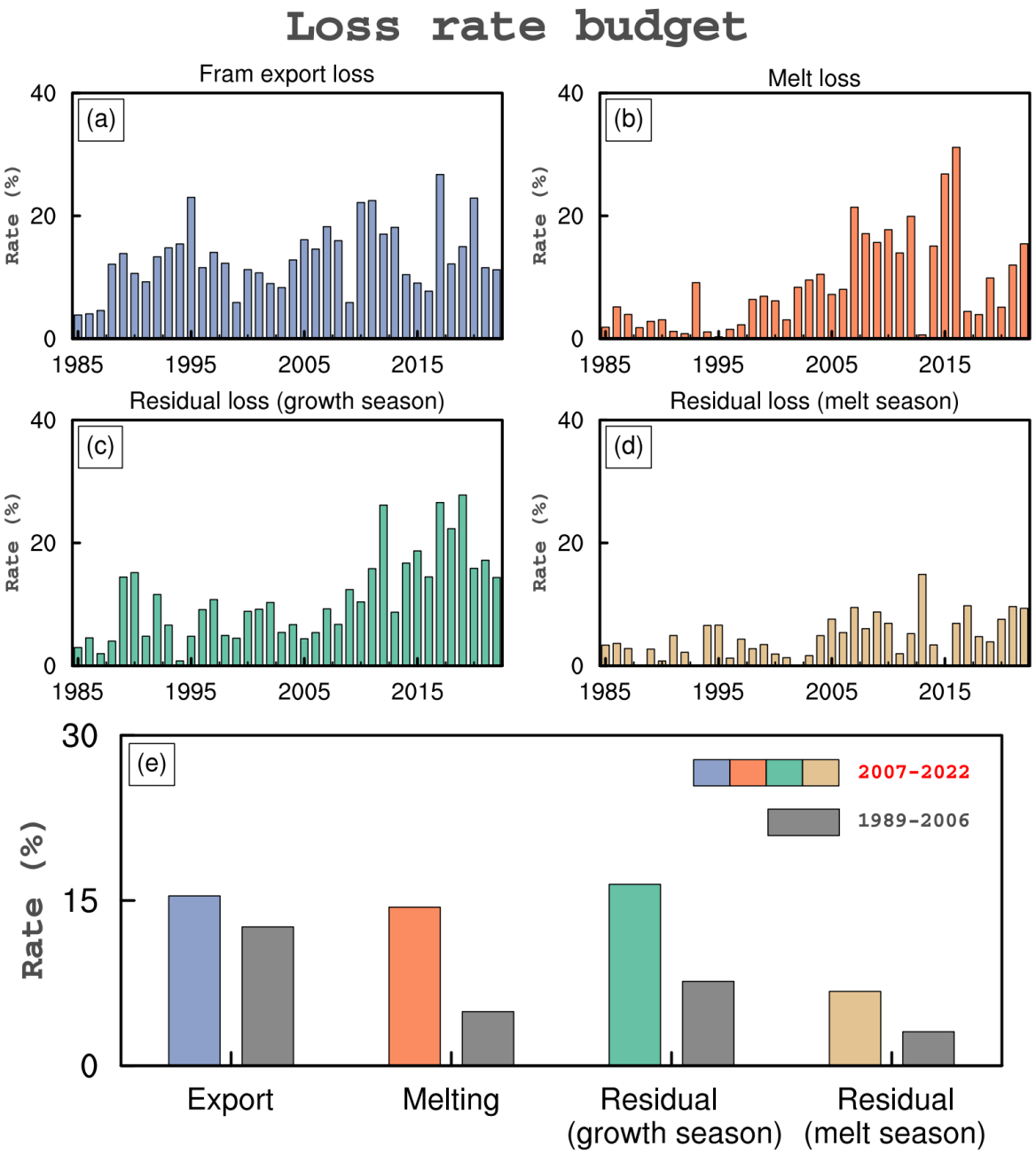

Figure 5. The 3+ year ice loss rate during 1985–2022 contributed by (a) export through FS, (b) summer melting, (c) residual part in the growth season and (d) residual part in the melt season. (e) Comparison in the average loss rate between 1989–2006 and 2007–2022.

https://doi.org/10.1017/jog.2024.33 Published online by Cambridge University Press

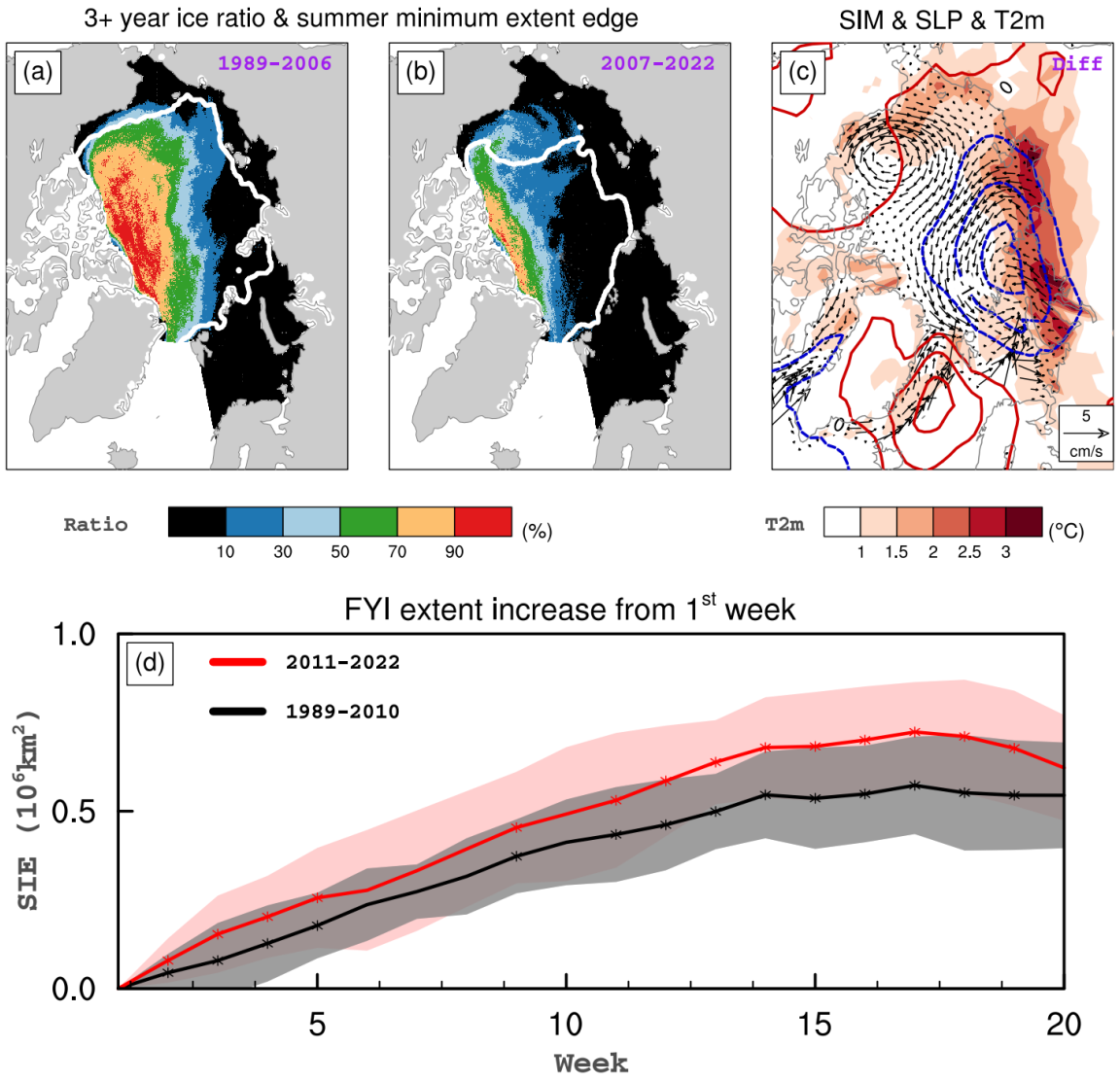

Figure 6. (a, b) The ratio of each grid cell occupied by 3+ year ice at the onset of melt season (20th–25th weeks) during (a) 1989–2006 and (b) 2007–2022. The white line indicates the averaged summer minimum SIE during corresponding periods. (c) The difference of SIM (vectors) and sea level pressure averaged over January–May (contours), and 2m air temperature averaged over August–September (shading) between 2007–2022 and 1989–2006. (d) The increase of FYI extent from 1st week (1–7 January) averaged over 2011–2022 (red line) and 1989–2010 (black line). The asterisks indicate where their difference is significant ($p < 0.1$; two-sample t-test). The shadings represent the range of range of one standard deviation.

https://doi.org/10.1017/jog.2024.33 Published online by Cambridge University Press

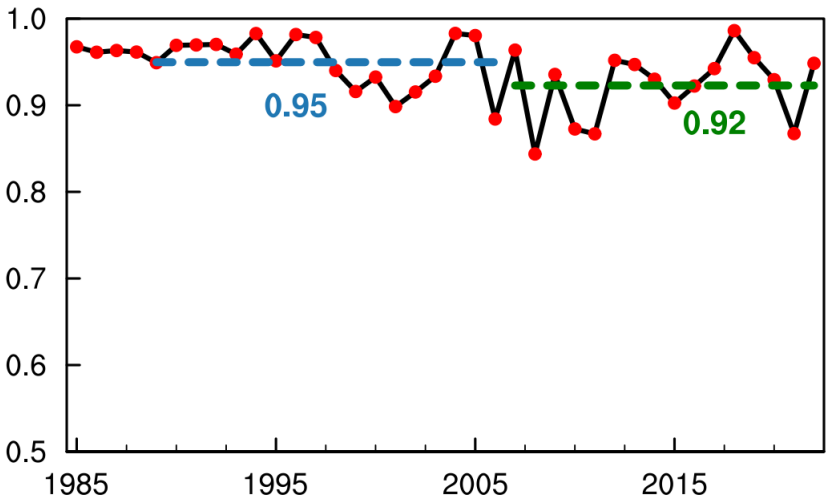

Figure 7. The ratio of 3+ year ice pixels with their SIC greater than 50% relative to the total 3+ year ice pixels in the start week. Blue and green dash lines indicate the averages for 1989–2006 and 2007–2022, respectively.

Acknowledgments

This study was supported by the National Key Research and Development Program of China (Grant No. 2022YFE0106800), the Natural Science Foundation of China (NSFC) (Grants Nos. 42230603), and the Innovation Group Project of the Southern Marine Science and Engineering Guangdong Laboratory (Zhuhai) (Grant No. 311021001). We thank David Babb and one anonymous reviewer for their careful reading of our manuscript and their insightful suggestions.

References

Armour KC, Bitz CM, Thompson L and Hunke EC (2011) Controls on Arctic Sea Ice from First-Year and Multiyear Ice Survivability. *Journal of Climate* **24**(9), 2378–2390. doi:10.1175/2010JCLI3823.1.

Babb DG and 8 others (2023) The Stepwise Reduction of Multiyear Sea Ice Area in the Arctic Ocean Since 1980. *Journal of Geophysical Research: Oceans* **128**(10), e2023JC020157. doi:10.1029/2023JC020157.

Babb DG, Galley RJ, Howell SEL, Landy JC, Stroeve JC and Barber DG (2022) Increasing Multiyear Sea Ice Loss in the Beaufort Sea: A New Export Pathway for the Diminishing Multiyear Ice Cover of the Arctic Ocean. *Geophysical Research Letters* **49**(9), e2021GL097595. doi:10.1029/2021GL097595.

Belchansky GI, Douglas DC and Platonov NG (2004) Duration of the Arctic Sea Ice Melt Season: Regional and Interannual Variability, 1979–2001. *Journal of Climate* **17**(1), 67–80. doi:10.1175/1520-0442(2004)017<0067:DOTASI>2.0.CO;2.

Bi H and 9 others (2020) Arctic multiyear sea ice variability observed from satellites: a review. *Journal of Oceanology and Limnology* **38**(4), 962–984. doi:10.1007/s00343-020-0093-7.

Comiso JC (2012) Large Decadal Decline of the Arctic Multiyear Ice Cover. *Journal of Climate* **25**(4), 1176–1193. doi:10.1175/JCLI-D-11-00113.1.

DiGirolamo NE, Parkinson CL, Cavalieri DJ, Gloersen P and Zwally HJ (2022) Sea Ice Concentrations from Nimbus-7 SMMR and DMSP SSM/I-SSMIS Passive Microwave Data, Version 2. Boulder, Colorado USA. NASA National Snow and Ice Data Center Distributed Active Archive Center. doi:10.5067/MPYG15WAA4WX.

Francis JA and Wu B (2020) Why has no new record-minimum Arctic sea-ice extent occurred since September 2012? *Environmental Research Letters* **15**(11), 114034. doi:10.1088/1748-9326/abc047.

Hersbach H and 42 others (2020) The ERA5 global reanalysis. *Quarterly Journal of the Royal Meteorological Society* **146**(730), 1999–2049. doi:10.1002/qj.3803.

Korosov AA and others (2018) A new tracking algorithm for sea ice age distribution estimation. *The Cryosphere* **12**(6), 2073–2085. doi:10.5194/tc-12-2073-2018.

Krumpen T and others (2019) Arctic warming interrupts the Transpolar Drift and affects long-range transport of sea ice and ice-rafted matter. *Scientific Reports* **9**(1), 5459. doi:10.1038/s41598-019-41456-y.

Kwok R (2018) Arctic sea ice thickness, volume, and multiyear ice coverage: losses and coupled variability (1958–2018). *Environmental Research Letters* **13**(10), 105005. doi:10.1088/1748-9326/aae3ec.

Kwok R (2015) Sea ice convergence along the Arctic coasts of Greenland and the Canadian Arctic Archipelago: Variability and extremes (1992–2014). *Geophysical Research Letters* **42**(18), 7598–7605. doi:10.1002/2015GL065462.

Kwok R (2007) Near zero replenishment of the Arctic multiyear sea ice cover at the end of 2005 summer. *Geophysical Research Letters* **34**(5). doi:10.1029/2006GL028737.

Kwok R and Cunningham GF (2010) Contribution of melt in the Beaufort Sea to the decline in Arctic multiyear sea ice coverage: 1993–2009. *Geophysical Research Letters* **37**(20). doi:10.1029/2010GL044678.

Liu J and 13 others (2019) Towards reliable Arctic sea ice prediction using multivariate data assimilation. *Science Bulletin* **64**(1), 63–72. doi:10.1016/j.scib.2018.11.018.

Mallett RDC and 9 others (2021) Record winter winds in 2020/21 drove exceptional Arctic sea ice transport. *Communications Earth & Environment* **2**(1), 1–6. doi:10.1038/s43247-021-00221-8.

Maslanik J, Stroeve J, Fowler C and Emery W (2011) Distribution and trends in Arctic sea ice age through spring 2011. *Geophysical Research Letters* **38**(13). doi:10.1029/2011GL047735.

Maslanik J and 6 others (2007) A younger, thinner Arctic ice cover: Increased potential for rapid, extensive sea-ice loss. *Geophysical Research Letters* **34**(24). doi:10.1029/2007GL032043.

Moore GWK, Steele M, Schweiger AJ, Zhang J and Laidre KL (2022) Thick and old sea ice in the Beaufort Sea during summer 2020/21 was associated with enhanced transport. *Communications Earth & Environment* **3**(1), 1–11. doi:10.1038/s43247-022-00530-6.

Notz D and Marotzke J (2012) Observations reveal external driver for Arctic sea-ice retreat. *Geophysical Research Letters* **39**(8). doi:10.1029/2012GL051094.

Perovich D and 6 others (2013) Sea Ice [in Arctic Report Card 2013]. *Arctic Report Card 2013*.

Polyakov IV and 7 others (2023) Fluctuating Atlantic inflows modulate Arctic atlantification. *Science* **381**(6661), 972–979. doi:10.1126/science.adh5158.

Rampal P, Weiss J and Marsan D (2009) Positive trend in the mean speed and deformation rate of Arctic sea ice, 1979–2007. *Journal of Geophysical Research: Oceans* **114**(C5). doi:10.1029/2008JC005066.

Regan H, Rampal P, Ólason E, Boutin G and Korosov A (2023) Modelling the evolution of Arctic multiyear sea ice over 2000–2018. *The Cryosphere* **17**(5), 1873–1893. doi:10.5194/tc-17-1873-2023.

Sumata H, De Steur L, Divine DV, Granskog MA and Gerland S (2023) Regime shift in Arctic Ocean sea ice thickness. *Nature* **615**(7952), 443–449. doi:10.1038/s41586-022-05686-x.

Thomas DN (2017) *Sea ice.*, Third edition. John Wiley & Sons, Chichester, UK ; Hoboken,

NJ.

Tilling RL, Ridout A, Shepherd A and Wingham DJ (2015) Increased Arctic sea ice volume after anomalously low melting in 2013. *Nature Geoscience* **8**(8), 643–646. doi:10.1038/ngeo2489.

Tooth M and Tschudi M (2018) Investigating Arctic Sea Ice Survivability in the Beaufort Sea. *Remote Sensing* **10**(2), 267. doi:10.3390/rs10020267.

Tschudi MA, Meier WN and Stewart JS (2020) An enhancement to sea ice motion and age products at the National Snow and Ice Data Center (NSIDC). *The Cryosphere* **14**(5), 1519–1536. doi:10.5194/tc-14-1519-2020.

Tschudi MA, Meier W, Stewart J, Fowler C and Maslanik J (2019a) EASE-Grid Sea Ice Age, Version 4. Boulder, Colorado USA. NASA National Snow and Ice Data Center Distributed Active Archive Center. doi:10.5067/UTAV7490FEPB.

Tschudi MA, Meier W, Stewart J, Fowler C and Maslanik J (2019b) Polar pathfinder daily 25 km EASE-grid sea ice motion vectors, version 4. Boulder, Colorado USA. NASA National Snow and Ice Data Center Distributed Active Archive Center. doi:10.5067/INAWUWO7QH7B.

Tschudi MA, Stroeve JC and Stewart JS (2016) Relating the Age of Arctic Sea Ice to its Thickness, as Measured during NASA's ICESat and IceBridge Campaigns. *Remote Sensing* **8**(6), 457. doi:10.3390/rs8060457.

Wang Y, Bi H and Liang Y (2022) A Satellite-Observed Substantial Decrease in Multiyear Ice Area Export through the Fram Strait over the Last Decade. *Remote Sensing* **14**(11), 2562. doi:10.3390/rs14112562.

Yang Y, Min C, Luo H, Kauker F, Ricker R and Yang Q (2023) The evolution of the Fram Strait sea ice volume export decomposed by age: estimating with parameter-optimized sea ice-ocean model outputs. *Environmental Research Letters* **18**(1), 014029. doi:10.1088/1748-9326/acaf3b.

Ye Y and 8 others (2023) Inter-comparison and evaluation of Arctic sea ice type products. *The Cryosphere* **17**(1), 279–308. doi:10.5194/tc-17-279-2023.

Zhang J (2021) Recent Slowdown in the Decline of Arctic Sea Ice Volume Under Increasingly Warm Atmospheric and Oceanic Conditions. *Geophysical Research Letters* **48**(18), e2021GL094780. doi:10.1029/2021GL094780.

Zhang J, Lindsay R, Schweiger A and Rigor I (2012) Recent changes in the dynamic properties of declining Arctic sea ice: A model study. *Geophysical Research Letters* **39**(20). doi:10.1029/2012GL053545.

Zhao J, He S, Fan K, Wang H and Li F (2023) Projecting Wintertime Newly Formed Arctic Sea Ice Through Weighting CMIP6 Model Performance and Independence. *ADVANCES IN ATMOSPHERIC SCIENCES* **40**, 1–18. doi:10.1007/s00376-023-2393-2.